

## SUPPORTING INFORMATION

### ➤ **Synthesis of MCF silica**

Mesocellular foam (MCF) silica has been chosen as adsorbent support due to its large spherical pore size ( $>8$  nm), large surface area ( $>500$  m<sup>2</sup>/g), narrow pore size distribution, large pore volume ( $>1.5$  cm<sup>3</sup>/g) and three-dimensional pore structure (1-4). MCF silica was synthesized according to the procedures described in the literature (1-5). A triblock copolymer of poly(ethylene glycol) and poly(propylene glycol) (Pluronic P123, EO<sub>20</sub>PO<sub>70</sub>EO<sub>20</sub>, Sigma Aldrich) was used as a structure-directing agent, tetraethoxysilane (TEOS, Sigma Aldrich) as a silica source, 1,3,5-trimethyl benzene (mesitylene, Alfa Aesar) as a swelling agent, and K<sub>2</sub>SO<sub>4</sub> (Sigma Aldrich) as a strong electrolyte. K<sub>2</sub>SO<sub>4</sub> is used to prevent agglomeration and to form highly dispersed particles (1). Firstly, 2 g of Pluronic P123 and a certain amount of K<sub>2</sub>SO<sub>4</sub> salt (1:1 ratio of salt to TEOS) were dissolved in a 1.7M HCl (aq). Once the solution became transparent, 1.5 g of mesitylene was slowly added to this solution under continuous mixing. After 2 hours, 4.3 g of TEOS was added dropwise under vigorous stirring. The resulting solution was left under static conditions at 40°C for 24 hours and then transferred to a Teflon-lined autoclave and hydrothermally treated at 100°C for 48 hours. The product was subsequently filtered, washed with DI water/ethanol solution, dried in the air, and calcined at 550°C (1°C/min heating rate, 6 hours holding time) to remove the occluded organics and water.

### ➤ **Functionalization of adsorbent supports with mercaptan groups**

Silica was functionalized with mercaptan groups in dry toluene (99.5%, Alfa Aesar) by reacting with (3-mercaptopropyl)-trimethoxysilane (MPTMS, 95%, Sigma Aldrich) according to the procedure described in the literature (6-8). Before the functionalization, silica was acid-washed

by refluxing it in 0.2 M HCl (ACS Grade, Fisher Chemical) for four hours to remove surface residues and increase the surface density of silanol groups (9). The resulting acid-washed (AW) silica was dried in vacuum at 60° for 12 hours. MPTMS-silica was prepared by reacting the AW silica with (3-mercaptopropyl)-trimethoxysilane (MPTMS, 95%, SigmaAldrich) in dry toluene (99.5%, Alfa Aesar) according to the procedure described in the literature (6-8). 4 grams of AW silica were dispersed in 60 mL of dry toluene to which 16 mmol of MPTMS was slowly added. The mixture was refluxed for 24 hours under argon gas to avoid oxidation of mercaptan groups into disulfide moieties (7). The resulting product, MPTMS-silica, was filtered, washed with toluene solvent, and dried under vacuum at 60°C for 12 hours.

➤ **Thermodynamic calculations using DMol<sup>3</sup>**

Theoretical thermodynamic properties of a structure in Dmol<sup>3</sup> are calculated using the results of a vibrational analysis, which consists of various translational, rotational, and vibrational components at finite temperatures (10).

The following formulas used for thermodynamic calculations are based on the work by Hirano (11).

The enthalpy correction,  $H(T)$ , in the ideal gas is given by:

$$H(T) = E_{vib}(T) + E_{rot}(T) + E_{trans}(T) + RT$$

where R is the ideal gas constant and the subscripts represent vibrational, rotational, and translational contributions, respectively.

$$E_{trans} = \frac{3}{2}RT; E_{rot}(linear) = RT; E_{rot}(nonlinear) = \frac{3}{2}RT;$$

$$E_{vib} = \frac{R}{k} \sum_i \frac{h\nu_i}{2} + \frac{R}{k} \sum_i \frac{h\nu_i \exp\left(-\frac{h\nu_i}{kT}\right)}{\left[1 - \exp\left(-\frac{h\nu_i}{kT}\right)\right]}$$

where  $k$  is the Boltzmann constant,  $h$  is the Planck constant, and  $\nu_i$  are the individual vibrational frequencies.

The contributions to the entropy  $S$  are given by:

$$S_{trans} = \frac{5}{2}R \ln T + \frac{3}{2}R \ln \omega - R \ln p - 2.31482$$

$$S_{rot}(linear) = R \ln \left[ \frac{8\pi^2 I k T}{\sigma h^2} \right] + R$$

$$S_{rot}(nonlinear) = \frac{R}{2} \ln \left[ \frac{\pi^3 8\pi^2 c I_A 8\pi^2 c I_B 8\pi^2 c I_C (k_B T)^3}{\sigma^2 h^3 (hc)^3} \right] + \frac{3}{2}R$$

$$C_{vib} = R \sum_i \frac{\frac{h\nu_i}{k_B T} \exp\left(-\frac{h\nu_i}{k_B T}\right)}{1 - \exp\left(-\frac{h\nu_i}{k_B T}\right)} - R \sum_i \ln \left[ 1 - \exp\left(-\frac{h\nu_i}{k_B T}\right) \right]$$

where  $\omega$  is the molecular weight,  $I_x$  is the moment of inertia about axis  $x$ .

The energy calculations in DMol<sup>3</sup> provide the total electronic energy at 0 K. The thermodynamic analysis from DMol<sup>3</sup> provides the corrections for  $H$ ,  $S$ , and  $G$  at finite temperatures.

**Table S.1. The composition of simulated FGD wastewater**

Ion	Target Concentration ( $\mu\text{g/L}$ )
$\text{NO}_3^-$	60,000
$\text{Na}^+$	3,108,251
RF Power	1550 W
$\text{SO}_4^{2-}$	5,153,670
Sample depth	8 mm
$\text{Cd}(\text{NO}_3)_2$	28
Carrier gas flow	$1 \text{ L min}^{-1}$
$\text{Na}_2\text{SeO}_4$	404
Spray chamber type	Double pass
$\text{Na}_2\text{HAsO}_4$	89
Nebulizer type	Microconcentric
$\text{TiNO}_3$	61
Nebulizer pump	$0.1 \text{ lps}$
$\text{Pb}(\text{NO}_3)_2$	200

**Table S.2. Typical operating conditions and instrumental parameters for  $\text{Hg}^{2+}$  concentration measurements by ICP-MS**

**Table S.3. DMol<sup>3</sup> calculation parameters**

<b>Calculate</b>	optimize
<b>Opt_energy_convergence</b>	1.00E-05
<b>Opt_gradient_convergence</b>	2.00E-03 A
<b>Opt_displacement_convergence</b>	5.00E-03 A
<b>Opt_iterations</b>	50
<b>Opt_max_displacement</b>	0.3 A
<b>Symmetry</b>	off
<b>Max_memory</b>	7000
<b>File_usage</b>	smart
<b>Scf_density_convergence</b>	1.00E-06
<b>Scf_charge_mixing</b>	1.00E-01
<b>Scf_spin_mixing</b>	1.00E-01
<b>Scf_diis</b>	7 pulay
<b>Scf_iterations</b>	100
<b>Spin_polarization</b>	unrestricted
<b>Charge</b>	2
<b>Basis</b>	dnp
<b>basis_version</b>	basfile_v4.4
<b>Pseudopotential</b>	vpsr
<b>Functional</b>	pbe
<b>Aux_density</b>	hexadecapole
<b>Dftd</b>	TS
<b>Integration_grid</b>	fine
<b>Occupation</b>	Thermal 0.001
<b>Cutoff_Global</b>	4.6 Angstrom
<b>Cosmo</b>	ibs
<b>COSMO_Dielectric</b>	78.54 Water
<b>Kpoints</b>	off

**Figure S.1. TGA curve of MPTMS functionalized SG silica in air**

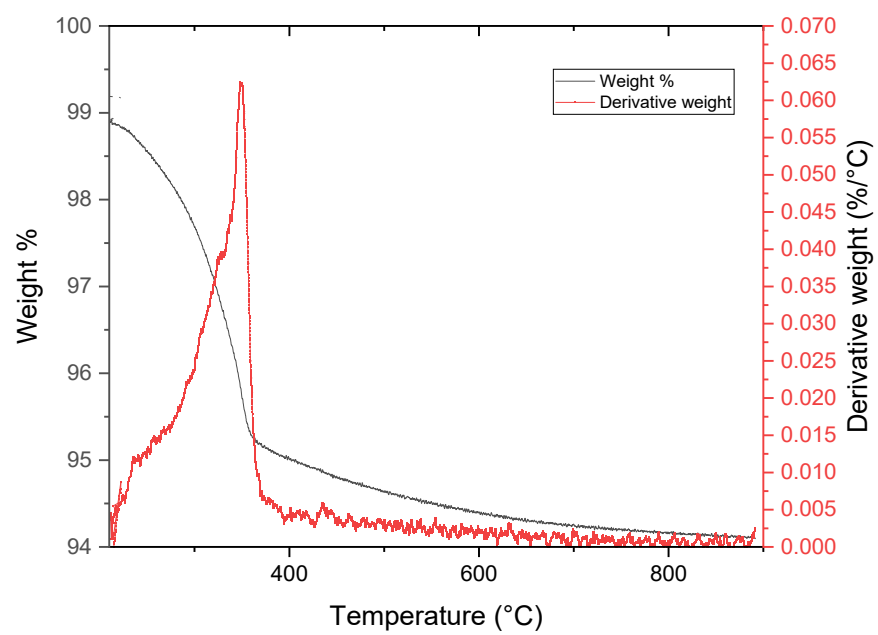


**Figure S.2. TGA curve of MPTMS functionalized Davisil silica in air**

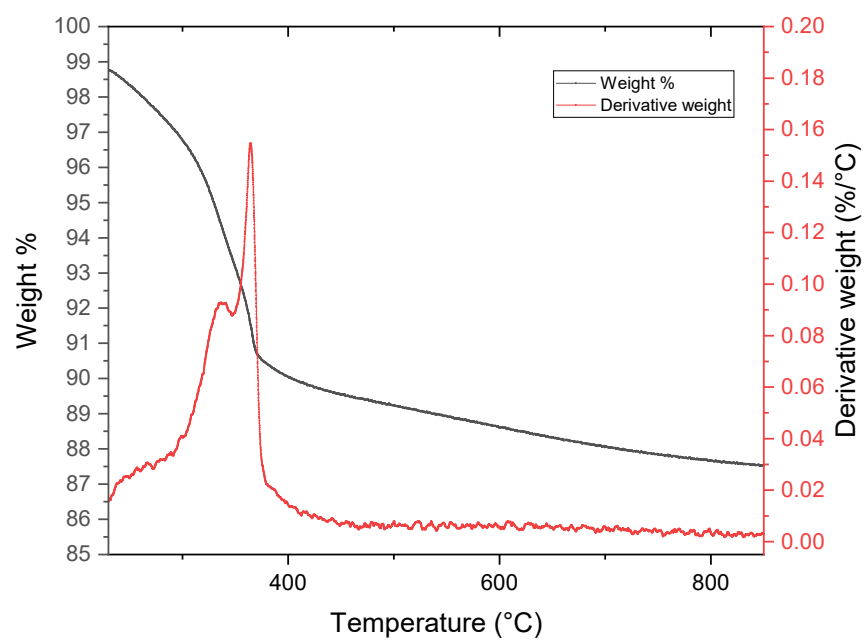


**Figure S.3. TGA curve of MPTMS functionalized MCF silica in air**

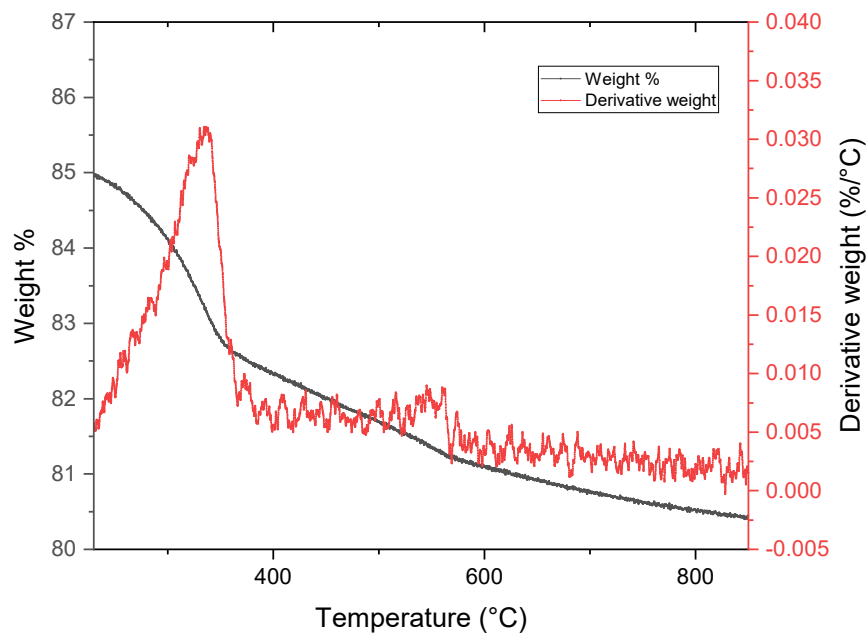
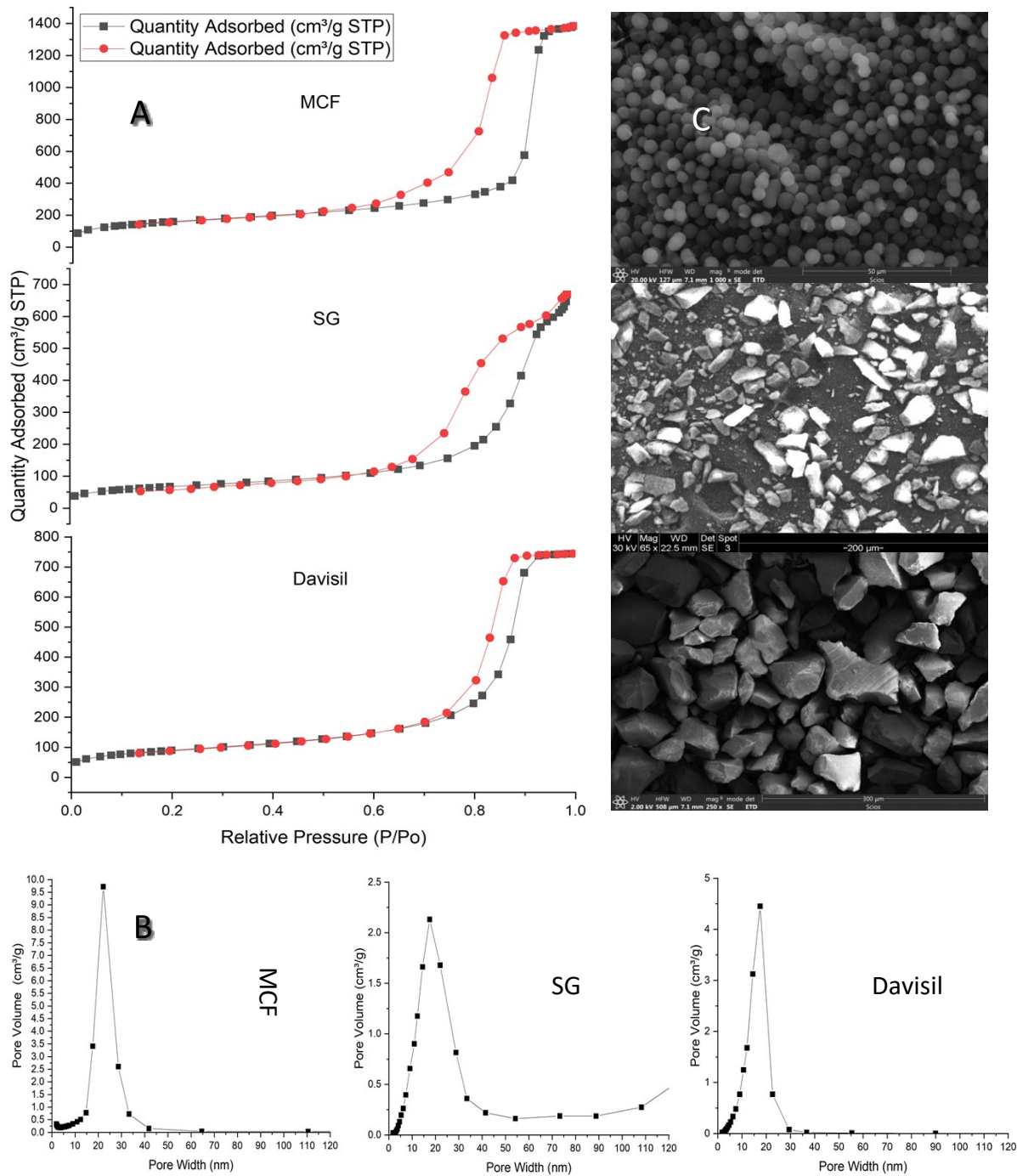


Fig. S.4 shows the N<sub>2</sub> adsorption-desorption isotherms of MCF, Davisil, and SG silicas employed in this study. All three silicas are characterized by a pore condensation and hysteresis behavior, indicated by type IV(a) N<sub>2</sub> adsorption/desorption isotherm per IUPAC classification (12), generally given to mesoporous materials. However, these silica supports do not exhibit the same hysteresis loop. The MCF and Davisil silica show very steep desorption branches characteristic of the H2(a) loop, which can be ascribed to either pore-blocking or a cavitation-induced evaporation (12). On the other hand, the SG silica exhibited a type H2(b) loop, which is associated with pore-blocking and wide distribution of pore diameter values. These conclusions are also consistent with the pore size distribution of these silica supports shown in Figure S.4(b). On the other hand, the pore size distribution of the SG silica appears to be wider, with much larger pore diameters present. Figure S.4(c) also shows the SEM images of the silica supports with MCF silica exhibiting uniform



spherical morphology with an average size of 10  $\mu\text{m}$ , whereas the Davisil and SG silica displayed irregular agglomerates with an average size of 50 and 200  $\mu\text{m}$ , respectively.



**Figure S.4.** a) N<sub>2</sub> adsorption-desorption isotherms and pore size distributions of MCF, Davisil, and SG silicas. b) Pore distribution using the BJH model for the adsorption branch of the nitrogen isotherm of silicas at 77 K. c) SEM images of MCF (top), SG (middle), and Davisil (bottom) silicas.

The successful surface attachment of MPTMS groups was confirmed by the XPS analysis (Figure S.5). High-resolution XPS spectra of S 2p core level for the *in situ* outgassed MPTMS-Davisil sample revealed a characteristic S 2p<sub>3/2</sub>-S 2p<sub>1/2</sub> spin-orbital splitting. The S fitting spectra of the MPTMS-Davisil silica showed a 2p<sub>1/2</sub> peak at 164.9 eV, corresponding to mercaptan groups (13, 14). No peaks corresponding to oxidized sulfonic species were observed in this sample (a typical value for S 2p core peak is 168.5 eV for -SO<sub>3</sub>H) (11, 12). This finding strongly confirmed the presence of the mercaptan groups on the surface of the functionalized adsorbent.

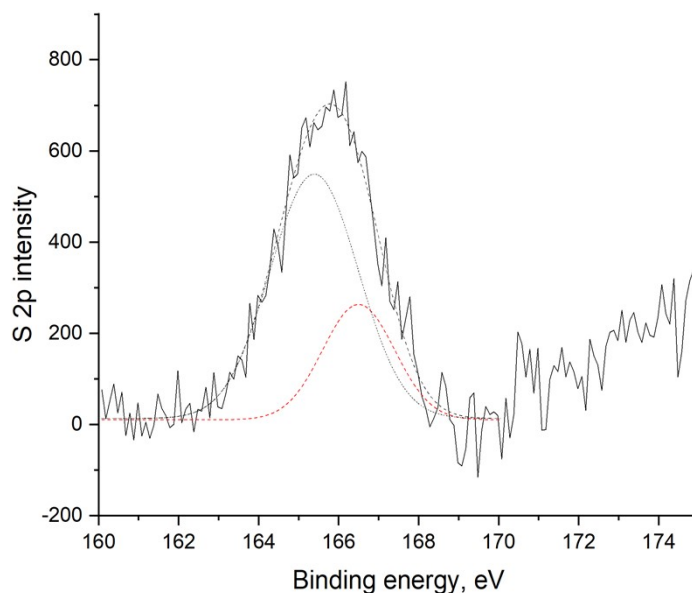


**Figure S.5.** S 2p XPS spectrum of MPTMS-Davisil silica. Blackline is the raw data; dotted lines denote individual fit components (166.2 eV and 164.5 eV characteristic of 2p<sub>3/2</sub> and 2p<sub>1/2</sub> for mercaptan groups).

## References

- (1) Chen, S.; Zhang, X.; Han, Q.; Ding, M. Y. Synthesis of highly dispersed mesostructured cellular foam silica sphere and its application in high-performance liquid chromatography. *Talanta (Oxford)* **2012**, *101*, 396-404, DOI: 10.1016/j.talanta.2012.09.047.
- (2) Santos, S. M. L.; Cecilia, J. A.; Vilarrasa-García, E.; Silva Junior, I. J.; Rodríguez-Castellón, E.; Azevedo, D. C. S. The effect of structure modifying agents in the SBA-15 for its application in the biomolecules adsorption. *Microporous and Mesoporous Materials* **2016**, *232*, 53-64, DOI: 10.1016/j.micromeso.2016.06.004.
- (3) Xing, S.; Lv, P.; Fu, J.; Wang, J.; Fan, P.; Yang, L.; Yuan, Z. Direct synthesis and characterization of pore-broadened Al-SBA-15. *Microporous and Mesoporous Materials* **2017**, *239*, 316-327, DOI: 10.1016/j.micromeso.2016.10.018.
- (4) Schmidt-Winkel, P.; Lukens, W. W.; Zhao, D.; Yang, P.; Chmelka, B. F.; Stucky, G. D. Mesocellular Siliceous Foams with Uniformly Sized Cells and Windows. *Journal of the American Chemical Society* **1999**, *121*, 254-255, DOI: 10.1021/ja983218i.
- (5) Dong-Pyo Kim; Young-Kwon Oh; Lan-Young Hong; Yamini Asthana Synthesis of Super-hydrophilic Mesoporous Silica via a Sulfonation Route. *Journal of Industrial and Engineering Chemistry (Seoul, Korea)* **2006**, *12*, 911-917.
- (6) Walcarius, A.; Delacôte, C. Mercury(II) binding to thiol-functionalized mesoporous silicas: critical effect of pH and sorbent properties on capacity and selectivity. *Analytica Chimica Acta* **2005**, *547*, 3-13, DOI: 10.1016/j.aca.2004.11.047.
- (7) Delacôte, C.; Gaslain, F. O. M.; Lebeau, B.; Walcarius, A. Factors affecting the reactivity of thiol-functionalized mesoporous silica adsorbents toward mercury(II). *Talanta (Oxford)* **2009**, *79*, 877-886, DOI: 10.1016/j.talanta.2009.05.020.
- (8) Walcarius, A.; Etienne, M.; Lebeau, B. Rate of Access to the Binding Sites in Organically Modified Silicates. 2. Ordered Mesoporous Silicas Grafted with Amine or Thiol Groups. *Chemistry of Materials* **2003**, *15*, 2161-2173, DOI: 10.1021/cm021310e.
- (9) Kim, J.; Desch, R. J.; Thiel, S. W.; Guliants, V. V.; Pinto, N. G. Adsorption of biomolecules on mesostructured cellular foam silica: Effect of acid concentration and aging time in synthesis. *Microporous and Mesoporous Materials* **2012**, *149*, 60-68, DOI: 10.1016/j.micromeso.2011.08.031.
- (10) Dassault Système, Biovia *Materials Studio Online Help*; 2019;
- (11) Stewart, J.J.P. *MOPAC Manual, 7th Ed.*, 1993;
- (12) Thommes, M.; Kaneko, K.; Neimark, A. V.; Olivier, J. P.; Rodriguez-Reinoso, F.; Rouquerol, J.; Sing, K. S. W. Physisorption of gases, with special reference to the evaluation of

surface area and pore size distribution (IUPAC Technical Report). *Pure and Applied Chemistry* **2015**, *87*, 1051-1069, DOI: 10.1515/pac-2014-1117.

(13) Siril, P. F.; Shiju, N. R.; Brown, D. R.; Wilson, K. Optimising catalytic properties of supported sulfonic acid catalysts. *Applied Catalysis. A, General* **2009**, *364*, 95-100, DOI: 10.1016/j.apcata.2009.05.032.

(14) Cano-Serrano, E.; Blanco-Brieva, G.; Campos-Martin, J. M.; Fierro, J. L. G. Acid-Functionalized Amorphous Silica by Chemical Grafting—Quantitative Oxidation of Thiol Groups. *Langmuir* **2003**, *19*, 7621-7627, DOI: 10.1021/la034520u.